

# COMPARISON OF THE CONVERGENCE RATES BETWEEN FOURIER PSEUDOSPECTRAL AND FINITE VOLUME METHODS USING TAYLOR-GREEN VORTEX PROBLEM.

**Andreia Aoyagui Nascimento**  
**Felipe Pamplona Mariano**

Universidade Federal de Goiás  
andreaia@emc.ufg.br  
fpmariano@emc.ufg.br

**Elie Luis Martinez Padilla**

Universidade Federal de Uberlândia  
epadilla@mecanica.ufu.br

**Abstract.** *In the present work we show a brief description of the methods Fourier pseudospectral (FPM) and finite volumes (FVM). These methods are used for solving two-dimensional incompressible flows over non-cartesian bodies, using the Navier-Stokes equations and the immersed boundary method (IBM), where the IBM models the immersed bodies. The present study evaluates the accuracy and convergence rates of the FPM and FVM using the classical Taylor-Green vortex problem, flow of a decaying vortex. The results show that the FPM reaches third order of the convergence rate and the FVM second one. On the other hand, the computational time is higher in FPM simulations.*

**Keywords:** *Pseudospectral Method; Finite Volume Method; Immersed Boundary; Taylor-Green Vortex*

## 1. INTRODUCTION

The computational engineering, in particular computational fluid dynamics (CFD), is a fundamental tool to study the matter involving the flow, heat transfer, interaction fluid-structure. This in turn motivates considerable research efforts in complex phenomena modelling, to increase the field of investigation of computational applications.

The computational code is a tool to solve CFD problems. Then the computational code should not contain programming error. For this, it numerical techniques are suggested, this techniques are denominated verification. Kleijnen (1982) defined "Verification is determining that a simulation computer programs performs as intended, *i.e.*, debugging the computer program". This survey discusses testing and analysis techniques that can be used to validate software and to have confidence in the quality of the programming product (Adrian *et al.*, 1982).

This article discusses and compare the verification the two distinct numerical method which models a domain, and a methodology which describe a complex geometry inside on this. The methods used are Finite Volume Method (FVM) and Fourier Pseudospectral Method (FPM), geometry is modeled by Immersed Boundary. The computational code are two-dimensional, and analytical solution used was Taylor-Green equation, because the source term is zero (Mariano, 2011).

## 2. TAYLOR GREEN EQUATION

Taylor and Green, attempting to do connexion between the statistical representation of turbulence and dissipation of energy. In (Taylor and Green, 1937), the authors exposes a complete solution of the equations of motion, in sole special case will suffice to illustrate the process of refine grid of large eddies into smaller ones, based at velocity. The Eq.(1), Eq.(2) and Eq.(3), are the solution proposed by Taylor and Green (1937):

$$u = -U_{\infty} \cos(x) \cdot \sin(y) \cdot e^{-2.t.\nu} \quad (1)$$

$$v = U_{\infty} \sin(x) \cdot \cos(y) \cdot e^{-2.t.\nu} \quad (2)$$

$$P = \frac{U_{\infty}}{4} [\sin(2x) + \cos(2y)] \cdot e^{-4.t.\nu} \quad (3)$$

Where  $U_{\infty}$  is the flow velocity [m/s], x and y are axes coordinate [m], t is time variable, and  $\nu$  is the viscosity [m<sup>2</sup>/s]. The Fig.(1) shows the two fields of velocity, to analytical solutions of Eq.(1) and Eq.(2).

In Mariano (2007), Mariano *et al.* (2006) are showed that Eq.(1) and Eq.(2) content the continuity equation, and the Eq.(3) can be obtained by velocity analytical equations.

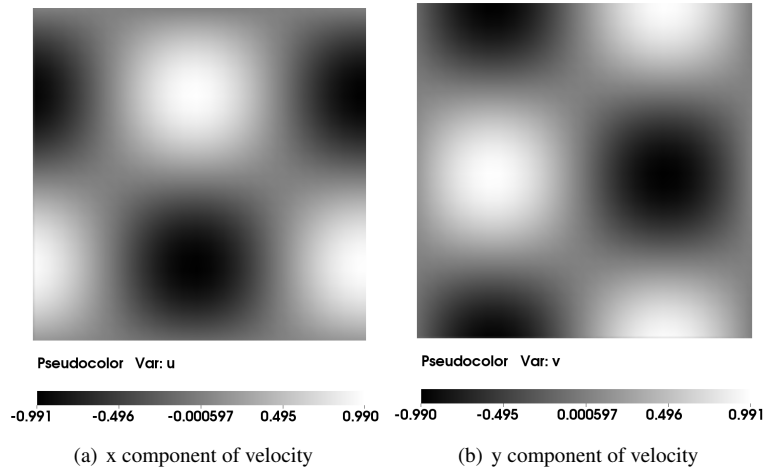


Figure 1: Field by velocity.

### 3. NUMERICAL METHODS

#### 3.1 Finite Volume Method

The finite volume method (FVM) is a discretization method which is well suited for the numerical simulation of various kinds of conservation laws, (Patankar, 1980). It is normally used in several engineering fields: fluid mechanics, heat and mass transfer, among others. This methodology is based on approach to physics of the problem represented by the Partial Differential Equations (PDE). The solution strategy of the FVM, is divide the domain into a number of control volume that corresponds to the mesh cells as Fig.(2) (Maliska, 1995; Patankar, 1980).

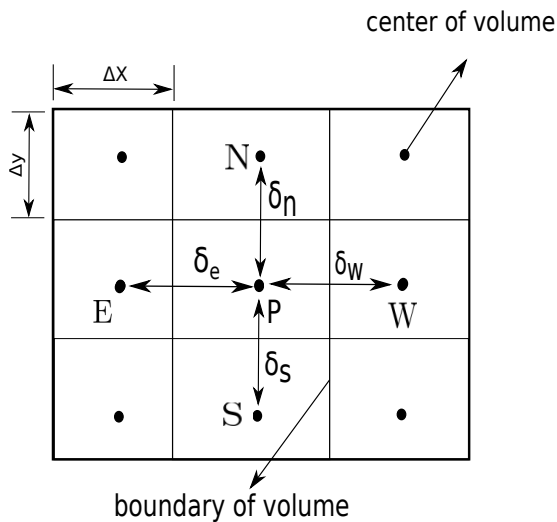


Figure 2: Scheme of the domain divisions performed with the finite volume method.

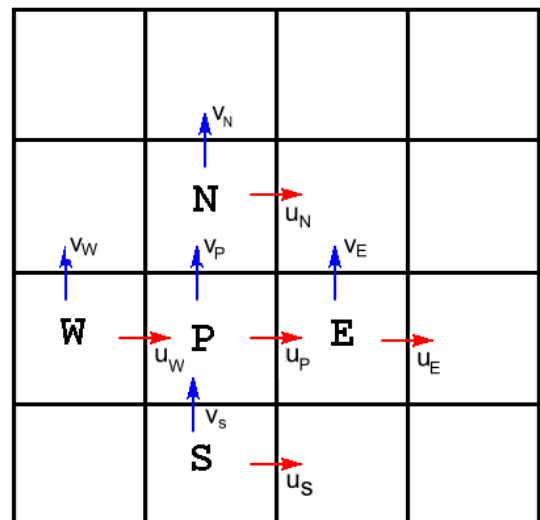


Figure 3: Scheme of the variable at the staggered mesh.

Figure (2) shows the scheme of the domain to FVM, where the  $E$  is east,  $W$  west,  $N$  north,  $S$  south and  $P$  is “central-volume” of the main mesh. The  $e, w, n, s$  refer to the face of this mesh; the  $\Delta x$  and  $\Delta y$  is the distance between the boundary volume and  $\delta_e, \delta_w, \delta_n$  and  $\delta_s$  are the distance between center of volumes.

In the present work, was used staggered mesh, which the pressure has the main mesh and the velocity are dislocate of  $\frac{\Delta x}{2}$  and  $\frac{\Delta y}{2}$ .

At Figure (3) represents the main mesh, where pressure and physical property are localized. The velocities are localized at the staggered mesh and are represented by red arrow (velocity at axes  $x$ ) and blue arrow (velocity at axes  $y$ ).

The finite volume method approximate equations are obtained through a balance of property involved conservation law, which are integrate at the control volume, Fig.(2). The Navier-Stokes equation at tensorial form, Eq.(4), is integrated

at space and time, Eq.(5) and Eq.(6).

$$\frac{\partial u_i}{\partial t} + \frac{\partial}{\partial x_j}(u_i u_j) = \frac{-1}{\rho} \frac{\partial P}{\partial x_i} + \nu \frac{\partial}{\partial x_j} \left( \frac{\partial u_i}{\partial x_j} \right) \quad (4)$$

$$\frac{u^t - u^0}{\Delta t} = \frac{P_e - P_w}{\Delta x} - \frac{u(u_e - u_w)}{\Delta x} - \frac{v(u_s - u_n)}{\Delta y} + \nu \left[ \left( \frac{U_E - U_P}{\delta_e} - \frac{U_P - U_W}{\delta_w} \right) \frac{1}{\Delta x} + \left( \frac{U_N - U_P}{\delta_n} - \frac{U_P - U_S}{\delta_s} \right) \frac{1}{\Delta y} \right] \quad (5)$$

$$\frac{v^t - v^0}{\Delta t} = \frac{P_n - P_s}{\Delta y} - \frac{v(v_e - v_w)}{\Delta y} - \frac{u(v_s - v_n)}{\Delta x} + \nu \left[ \left( \frac{V_E - V_P}{\delta_e} - \frac{V_P - V_W}{\delta_w} \right) \frac{1}{\Delta x} + \left( \frac{V_N - U_P}{\delta_n} - \frac{V_P - V_S}{\delta_s} \right) \frac{1}{\Delta y} \right] \quad (6)$$

In agreements with Souza (2005) this work uses the skew-simetric form due to stability. In Nascimento *et al.* (2012) is shown that the spacial derivates of the second orders FVM, has more error than time advance, and using central difference in the non-linear term is better than upwind scheme. So in this present work was used Euler to advance time and central difference to solve the non-linear term.

The Equation (5 - 6) are solved using the fractional step method to solve the pressure-velocity coupling, and the equations are solve by Gauss-Sidel method. The boundary condition is given, i.e. the velocity from analitical solution are applied at boundary.

### 3.2 Fourier Pseudospectral Method

Fourier Pseudospectral method (FPM) is based at solution at integration the term of Fourier series (DFT) along all discrete domain. The DFT is used to evaluate spatial derivatives in place of conventional finite volume. In according of Roache (1978) the use of the DFT over M nodepoints corresponds to using M-th order trigonometric interpolation to evaluate the derivatives. This procedure is of “infinite order”, in the sense that it may be shown to converge faster than any finite volume expression when all derivatives are continuous. Although it is, to require only periodic boundary condition.

FPM uses physical and spectral domains, which are co-related by reciprocity relation. The spectral methods applied to problems with smooth solutions attain high order of spatial convergency rates, because it use all collocation points to calculate a derivative in one point, (Basdevant, 1984; Canuto *et al.*, 2006; Briggs and Henson, 1995). The Eq.(4) at spectral domain is given by Eq.(7).

$$\frac{\partial \hat{u}_i}{\partial t} + ik_j (u_i * \hat{u}_j) = -ik_i \hat{P} - \nu k^2 \hat{u}_i \quad (7)$$

Where k is wave number, and  $k^2$  is,  $k^2 = k_j k_j$ ,  $\hat{u}_i$ , is the vector velocity transformed to Fourier space using the DFT, and  $i$  is the complex number  $\sqrt{-1}$ . It can be noted the convolution product at NLT  $ik_j (u_i * \hat{u}_j)$ , is used the Fourier pseudospectral method, (Canuto *et al.*, 2006; Souza, 2005; Mariano, 2007, 2011; Canuto *et al.*, 1988).

In order to uncouple the pressure and velocity at Eq.(7) was used the projection method. This method project the variables on plane, named plane  $\pi$ , which contains divergent of velocity null. For this, the plane  $\pi$  is perpendicular of vector wave number  $\vec{k}$  Canuto *et al.* (2006). The projection of pressure term transformed results at a point in this plane. Then in this method the pressure is condition to postprocessing.

The Equation (8) is the time discretization and Eq.(7) is the same equation projected on the plane  $\pi$ , where  $\wp(T\hat{N}\hat{L}_m^t)$  is non-linear term projected term.

$$\frac{\hat{u}_i^t - \hat{u}_i^0}{\Delta t} + \wp(T\hat{N}\hat{L}_m^t) = -\nu k^2 \hat{u}_i^t \quad (8)$$

### 3.3 Immersed Boundary

The term immersed boundary method, is used in present paper to reference a method developed by Peskin (1972), with the aim of simulated the cardiac mechanics valves and associated blood flow. Wherefore, is necessary use two domains, lagrangian and eulerian domain. The first is independent of eulerian domain, wich get model any object.

The Figure (4) represents the domain used to calculate the immersed boundary, where  $\vec{x}$  represents position any point at the field Eulerian ( $\Omega$ ) and  $\vec{X}$  position any point at the field Lagrangian ( $\Gamma$ ), (Peskin, 1972).

The verification using the IBM consist to put the analytical solution at lagrangian domain. This is possible using the source term  $f_i$ , which represents the force origin by IBM. Then for the Eulerian domain, Eq.(4) is Eq.(9).

$$\frac{\partial u_i}{\partial t} + \frac{\partial}{\partial x_j}(u_i u_j) = \frac{-1}{\rho} \frac{\partial P}{\partial x_i} + \nu \frac{\partial}{\partial x_j} \left( \frac{\partial u_i}{\partial x_j} \right) + f_i \quad (9)$$

The Direct-Forcing method (DFM) is used to calculate the Lagrangian field. The DFM developed by Mohd-Yusof (1997) extracts the forcing directly from the numerical solution, which is determined by difference between the interpolated velocities in the boundary points and the desired at the physical boundary velocities. In this present work was chosen

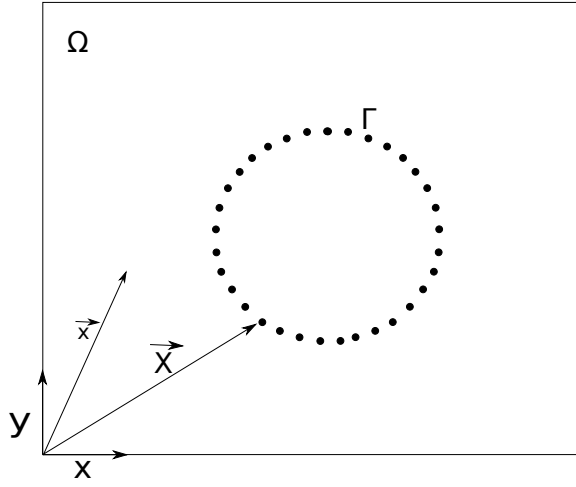


Figure 4: Scheme of eulerian and lagrangian mesh.

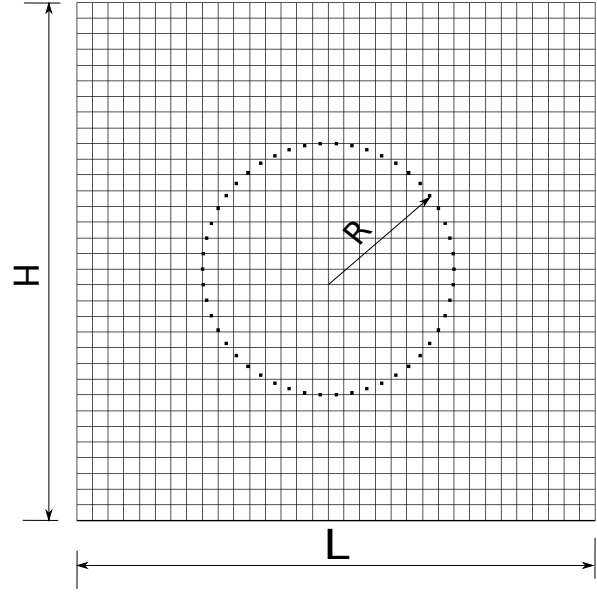


Figure 5: Scheme of Immersed boundary method.

direct-forcing, due to low difficulty implementation and the good results (Mariano, 2007, 2011; Moreira, 2011). In This methodology, both domains (Lagrangian and Eulerian) change informations using the Eq.(10).

$$f_x = \begin{cases} F_x(\vec{X}, t) & \text{if } \vec{x} = \vec{X} \\ 0 & \text{if } \vec{x} \neq \vec{X} \end{cases} \quad (10)$$

For the purpose of discussion of the general concepts, let us write the time-discretized at horizontal velocity component, Eq.(11), in the following form:

$$\frac{u^{t+\Delta t} - u^* + u^* - u^t}{\Delta t} + rhs + f_x = 0 \quad (11)$$

Where *rhs* regroups the convective and viscous terms at some intermediate time level between  $t$  and  $t+\Delta t$ . The Eulerian force term which yields the temporal parameter  $u^*$ . hen the Eq. (9) is solved in two steps, given by Eqs. (12) and (13) for both axes.

$$\frac{u^* - u^t}{\Delta t} + rhs = 0 \quad (12)$$

The lagrangian source term is given by Eq.(13) for  $X_l$ .

$$F_x = \frac{U^{t+\Delta t} - U^*}{\Delta t} \quad \forall X_l \quad (13)$$

Where  $U^{t+\Delta t}$  is the boundary condition and  $U^*$  is the temporal parameter interpolated. Lastly, the update by the eulerian velocity is given by Eq.( 14) where  $f_x$  is calculated by Eq.(9):

$$u^{t+\Delta t} = u^* + f_x \Delta t \quad (14)$$

It is possible if the Eulerian and Lagragian mesh are coincident, case the geometry is non coincident the force originated the immersed boundary have to be distributed. Peskin (1972) propose a function distribution is given by Eq.(16):

$$f_i(\vec{x}) = \sum_{\Gamma} D_h(\vec{x} - \vec{X}) F_i(\vec{X}) \Delta s^2 \quad (15)$$

$$D_h(\vec{x} - \vec{X}) = \frac{1}{h^2} W_g(r_x) W_g(r_y) \quad (16)$$

Where  $D_h$  is the distribution function,  $r_x = \frac{x-X}{\Delta x}$ ,  $r_y = \frac{y-Y}{\Delta y}$ ,  $\Delta s$  is distance of lagrangian points and  $W_g$  is the weight function.

$$W_{gc}(r) = \begin{cases} 1 - \frac{1}{2}|r| - |r|^2 + \frac{1}{2}|r|^3 & \text{if } 0 \leq |r| < 1; \\ 1 + \frac{11}{6}|r| + |r|^2 - \frac{1}{6}|r|^3 & \text{if } 1 \leq |r| < 2; \\ 0 & \text{if } 2 \leq |r|; \end{cases} \quad (17)$$

$$W_{gh}(r) = \begin{cases} 1 - |r| & \text{if } 0 \leq |r| < 1; \\ 0 & \text{if } 1 \leq |r|; \end{cases} \quad (18)$$

The major advantage of the discrete forcing is the absence of user specified parameters in calculate the force, and the elimination of associated stability constraints (Mittal and Iaccarino, 2005). Thus is possible to solve flows with complex geometry and maintain structured and uniform mesh, Fig.(5).

Figure (5) represents the problem domain two-dimensional simulated. Where, L and H are domain dimension, R is the radius of Lagrangian geometry. In Lagrangian mesh the velocity from analytical solution are introduce.

### 3.4 Simulation Parameter

The simulation was realized until  $t_a=0.3$ , where  $t_a$  is dimensionless time Eq.(19), likes Mariano (2007, 2011) used, and the time advance method is the Classic Runge-Kutta.

$$t_a = \frac{t}{2\pi} \quad (19)$$

The dimensional parameters are:

- $L = 2\pi$  [m],
- $H = 2\pi$  [m],
- $u_0 = 1.0$  [m/s] (reference velocity),
- $\rho = 1.0$  [Kg/m<sup>3</sup>] (specific mass),

The adimensionless parameters are:

- $Re = 100$  (Reynolds number),
- $N = 32, 64, 128$  and  $256$  (divisions number to H),
- $M = 32, 64, 128$  and  $256$  (divisions number to L),
- $CFL = 0,001$  (Curret number),

The convergence rate was obtained by  $L_2$  norm Eq.(20), where  $\phi_{ij}^a$  is the analitical variables and  $\phi_{ij}$  is the variables calculated:

$$L_2(\phi) = \sqrt{\frac{\sum_i^M \sum_j^N (\phi_{ij}^a - \phi_{ij})^2}{MN}} \quad (20)$$

## 4. RESULTS

Figure (6) and Figure (7) show fields of pressure, for two study method. In these figures can be noted the formation of counter-rotating vortex.

Figure (8) shows the order of convergency using the hat and cubic function distribution for the Finite Volume Method and Fourier Pseudospectral Method, where N is the divisions domain at a direction.

Figure(8 a)shows the rate convergence in the FVM, using the hat function (cross symbol), which tending the second order, *i.e.* the error from spatial discretization are bigger than interpolation error and distribution error. Using the cubic function (dash line) the results close to second order of convergency, which is, the discretization order of this method.

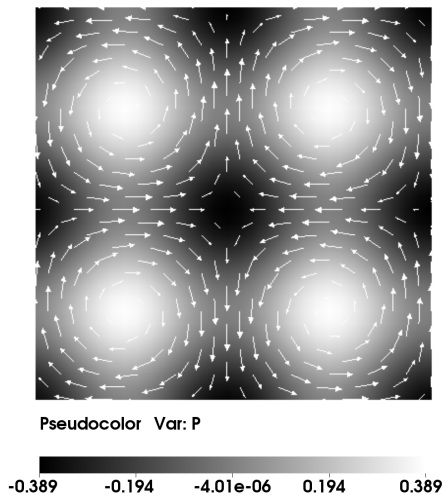


Figure 6: FPM couple IBM Direct-forcing method.

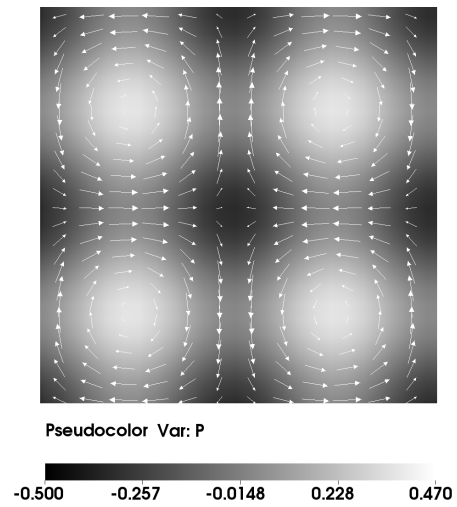
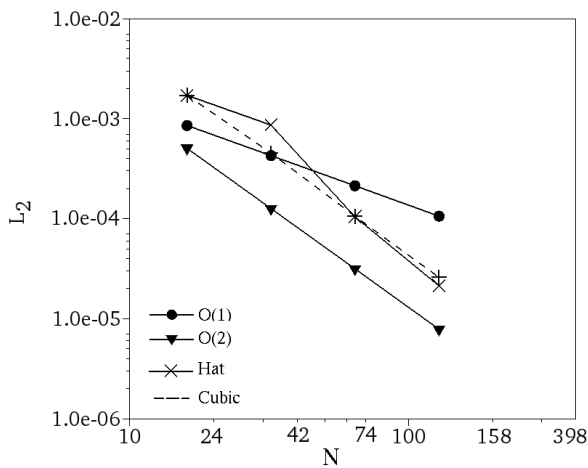
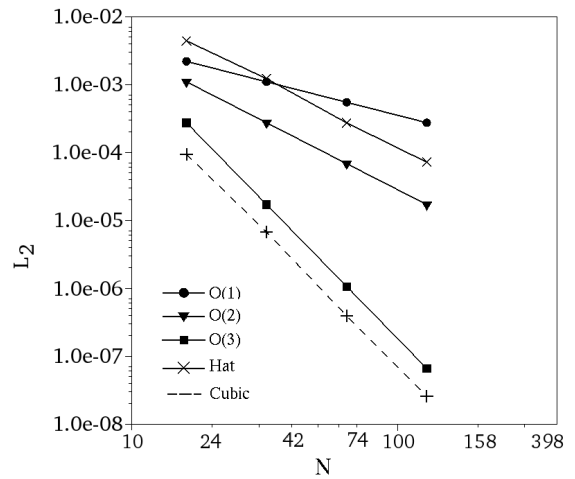


Figure 7: FVM couple IBM Direct-forcing method.



(a) Finite Volume Method



(b) Fourier Pseudospectral Method

Figure 8: Convergence rates.

Figure (8 b) shows the order of convergency for the Fourier Pseudospectral Method. In this note that using the Hat function (cross symbol), the solution close to the second order of converge, which is the order of the distribution function. The Cubic function (dash line) is the third order, although the FPM has high convergence order, in this case FPM has a limitation of the interpolation and distribution functions. Then, due to use the cubic function the FPM tending third order.

Table (1) is the computational time to solve the Navier-Stokes equation, using the Finite Volume Method and Fourier Pseudospectral Method, using the CPU processor AMD Phenom(tm) II X4 B97 Processor, RAM 7,3 Gib, 800,00 MHz and four core.

Table (1) shows values higher to FVM, this can be explained, because of the linear solver used to obtain the pressure field in FVM is the Gauss-Siedel. Aggrement of explained at section 3.2, the main characteristic of FPM is the projection of pressure field. This way, allows calculate the pressure field only to post-processing, which decreasing the computational time. It is highlight when increase the number of divisions, at domain.

Table 1: Computational time.

mesh	FPM	FVM
16	0.604909	0.604909
32	40.39186	25.506124
64	798.185658	3056.209385
128	14916.528343	160585.739258

## 5. CONCLUSION

The study of rate convergence at the numerical code is important because, the implementation errors can be found. Furthermore it shows the importance to use the interpolation scheme compatible with the spatial discretization.

In this work, the IBM is used to model non-cartesian geometries. This introduces numerical errors which affect the rate convergence of the FPM. Because the order of the interpolation and distribution functions are lower than FPM. But IBM is used in order to implementation of cylinder geometry in FPM.

Although using the IBM affects the accuracy and convergence in FPM, this method has good accuracy relative to FVM.

Next step, the study about influence of advanced time scheme will be performed, because using the FPM the Mariano *et al.* (2006) reached fourth order of same problem using the Runge Kutta Modified, and realized the validation using the cavity problem or circular Couette flow.

At attempting to obtain the better computational time for FVM, is suggested implementation of other solver to pressure, i.e. Strongly Implicit Procedure (SIP), and to obtain better accuracy to method, is suggested realize the improving (fourth order) discretization of the spatial derivatives.

Thus the FPM shows better accuracy and time computational than second order FVM, using Gauss-Siedel solver to Poisson equation to evaluate the pressure field, which justifies its use.

## 6. ACKNOWLEDGEMENTS

PETROBRÁS, CAPES, FAPEMIG, CNPQ and FAPEG for financial supports, Faculdade de Engenharia Mecânica of Universidade Federal de Uberlândia and Escola de Engenharia Elétrica, Mecânica e de Computação of Universidade Federal de Goiás.

## 7. REFERENCES

- Adriani, W.R., Branstad, M.A. and Cherniavsky, J.C., 1982. *Computing Surveys*, Vol. 14, pp. 159–192.
- Basdevant, C.e.a., 1984. “Spectral and finite difference solution of the burgers equation.” *Computers and Fluids*, pp. Vol. 14, No. 1, 23–41.
- Briggs, W. and Henson, V., 1995. *The DFT*. SIAM, Philadelphia.
- Canuto, C., Quarteroni, A., Hussaini, M.Y. and Zang, T.A., 1988. *Spectral methods in fluid dynamics 2nd*. Springer-Verlag, New York.
- Canuto, C., Quarteroni, A., Hussaini, M.Y. and Zang, T.A., 2006. *Spectral Methods-Fundamentals in Single Domains*. Springer, New York.
- Kleijnen, J.P., 1982. “Verification and validation of simulation models”. *European Journal of Operational Research*, Vol. 82, pp. 145–162.
- Maliska, C.R., 1995. *Transferência de calor e mecânica dos fluidos computacional*. Livros Técnicos e Científicos Editoras S.A. - LTC, Brasil.
- Mariano, F.P., 2007. “Simulação de escoamentos não-periódicos utilizando as metodologias pseudospectral e de fronteira imersa acopladas”.
- Mariano, F.P., 2011. “Soluções numéricas de Navier-Stokes utilizando uma hibridação das metodologias fronteira imersa e pseudospectral de Fourier”.
- Mariano, F.P., Moreira, L.Q. and Silveira-Neto, A., 2006. “Resolução de escoamentos não periódicos utilizando métodos pseudospectral e método da fronteira imersa”. Uberlândia, MG, Brazil.
- Mittal, R. and Iaccarino, G., 2005. “Immersed boundary methods”. *Annual Reviews of Fluids Mechanics*, pp. 239–261.
- Mohd-Yusof, J., 1997. “Combined immersed-boundary/b-spline methods for simulations of flow in complex geometries”. *CTR Annual Research Briefs*, pp. 317–327.
- Moreira, L.Q., 2011. “Modelagem matemática de jatos em desenvolvimento espacial usando a metodologia pseudospectral de Fourier”.
- Nascimento, A.A., Mariano, F.P. and Padilla, E.L.M., 2012. “Pseudospectral and finite volume solutions of burgers equation”. Rio de Janeiro, RJ, Brazil.
- Patankar, S.V., 1980. *Numerical Heat Transfer and Fluid Flow*. Taylor e FrancisBook LTD, USA.
- Peskin, C., 1972. “Flow patterns around heart valves: A numerical method”. *Journal of Computational Physics*, Vol. 10, pp. 252–271.
- Roache, P.J., 1978. “A pseudo-spectral FFT technique for non-periodic problems”. *Journal of Computational*, pp. 204–220.
- Souza, A.M., 2005. “Análise numérica da transição à turbulência em escoamentos de jatos circulares livres”.
- Taylor, G.I. and Green, A.E., 1937. “Mechanism of the production of small eddies from large ones”. Vol. 152, pp. 499–521.

## **8. RESPONSIBILITY NOTICE**

The authors are the only responsible for the printed material included in this paper.